DOI: 10.19884/j.1672-5220.202511008

A *Novosphingobium* Strain Capable of Degrading Cembratriene-4, 6-diol and Producing Aroma: Isolation, Identification and Biological Characterization

SHAO Xia[1], WANG Jiale[2], WU Da[2], ZHANG Zhe[1], SUN Yue[1], XING Jiayi[1], SHA Yunfei[2*]
1. Shanghai Institute of Technology, Shanghai 201418, China
2. The Key Laboratory of Cigarette Smoke, Shanghai Tobacco Group Co., Ltd., Shanghai 200082, China

Abstract: To obtain strains capable of efficient cembratriene-4,6-diol (CBT-diol) degradation for enhancing the tobacco aroma quality, a target strain designated as Z1-1 was isolated from tobacco leaves utilizing CBT-diol as the primary carbon source. Based on morphological characteristics, physiological biochemistry, and 16S rRNA gene sequence analysis, the strain was preliminarily identified as *Novosphingobium* sp. Through single-factor and response surface methodology experiments, the optimal degradation conditions were determined to be 30 ℃, 150 r/min shaking speed, 4% inoculum size, and pH 7.0. Under these optimized conditions, a CBT-diol degradation efficiency of 83.47% was achieved within 36 h. The application of this strain in tobacco concentrate significantly increased the relative contents of several key aroma components. The relative contents of solanone, 9-hydroxy-4, 7-megastigmatrienone, 4-hydroxy-β-damascone, and phytol increased to 7.22, 3.65, 1.79, and 3.80 times their original levels, respectively. These findings demonstrate that *Novosphingobium* sp. Z1-1 is an efficient CBT-diol-degrading and aroma-producing bacterium.

Keywords: cembratriene-4, 6-diol; *Novosphingobium* sp.; phylogenetic analysis; isolation and identification; degradation
CLC number: Q939.9 **Document code**: A
Article ID: 1672-5220(2026)03-0130-12

Open Science Identity (OSID)

0 Introduction

Cembranoids are important macrocyclic diterpenoid aroma precursors in tobacco, widely distributed in the glandular hair secretions on the surface of tobacco leaves, seeds, and floral organs[1]. Previous studies have reported that a total of 52 cembranoid compounds have been identified to date[2], among which cembratriene-4, 6-diol (CBT-diol) has the most prominent content, accounting for approximately 0.7% of the fresh weight of tobacco leaves and 40%–50% of the total lipids on the leaf surface[3-4]. In addition to exhibiting significant insecticidal and stress-resistance activities in plant defense[5-6], CBT-diol has also been confirmed to be closely related to human sensory responses[7-8].

During the curing and aging processes of tobacco, cembranoids can undergo a series of degradation reactions, generating a variety of key aroma components, including solanone, solanofuran, and norsolanadione[9-11]. Existing studies have shown that there are more than 60 degradation products, which play a decisive role in the formation of the characteristic aroma of tobacco. Therefore, systematically deciphering the degradation mechanism of cembranoids and rationally regulating their transformation pathways are of great practical value for improving the aroma quality of tobacco products.

The genus *Novosphingobium* and its phylogenetically related *sphingomonads* have shown broad potential in the fields of environmental bioremediation and organic waste resource utilization. In terms of resource recovery, *Novosphingobium* naphthalenivorans exhibits efficient degradation capacity for lignite from Chifeng, Inner Mongolia, with a degradation efficiency as high as 91.8%, providing a new idea for coal biotransformation[12]. In addition, *Sphingomonas*, a genus with similar properties to *Novosphingobium*, can significantly promote the decomposition of crop residues in reclaimed mining soils, accelerate the release of nutrients such as nitrogen, phosphorus, and potassium, and increase soil organic carbon content and key enzyme activities, thereby promoting the resource utilization of agricultural wastes and the restoration of soil fertility[13]. In the remediation of petroleum hydrocarbon pollution, *Novosphingobium* has been identified as a key functional genus for degrading petroleum hydrocarbons in oil-based drilling cuttings, and its metabolic activity and community structure are significantly regulated by the form of exogenous nitrogen[14]. The petroleum hydrocarbon components (such as alkanes and cycloalkanes) and CBT-diol share a hydrophobic main structure composed of a carbon-hydrogen framework. More importantly, the aliphatic long side chains in the CBT-diol molecule are similar to the alkane segments in

Received date: 2025-11-16
Foundation item: Open Project of the Key Laboratory of Cigarette Smoke, China National Tobacco Corporation (No. K2023-1-044P)
* Correspondence should be addressed to SHA Yunfei, e-mail: shayf@sh.tobacco.com.cn
Citation: Shao X, Wang J L, Wu D, et al. A *Novosphingobium* strain capable of degrading cembratriene-4,6-diol and producing aroma: isolation, identification and biological characterization [J]. *Journal of Donghua University (English Edition)*, 2026, 43(3): 130-141.

petroleum hydrocarbons, and their complex multi-ring terpenoid framework also shares common features in chemical inertness and spatial configuration with the cycloalkanes and multi-ring aromatic hydrocarbons in petroleum hydrocarbons. These structural similarities indicate that the key enzyme systems for degrading petroleum hydrocarbons (such as oxygenases and hydroxylases) may also apply to attacking similar sites in CBT-diol molecules due to their evolved ability to recognize and oxidatively break C—C bonds and ring structures. This provides a reasonable structural biological basis for using the known *Novosphingobium* genus bacteria, which have outstanding capabilities in degrading hydrocarbons in environmental remediation, to develop new functions in the targeted conversion of tobacco aroma precursors.

Currently, research on cembranoids mainly focuses on their pharmacological activities, such as anti-tumor and neuroprotective effects[15], while systematic studies on their biodegradation mechanisms under microbial action are still scarce. To improve the degradation efficiency of CBT-diol compounds and promote their directed transformation into aroma substances[16], this study takes *Novosphingobium* as the research object, aiming to identify the key factors affecting its degradation performance and provide a theoretical basis and technical support for the efficient improvement of the aroma quality of tobacco[15].

1 Materials and Methods

1.1 Materials

Tobacco leaf samples, including Honghuadajinyuan, Burley, K326, and Yunyan 87, were obtained from the Technology Center of Shanghai Tobacco Group Co., Ltd., China. CBT-diol (purity ≥ 99%) was purchased from Shanghai Huicheng Biotechnology Co., Ltd., China.

The culture media are as follows.

LB medium: tryptone (10 g/L), yeast extract (5 g/L), and NaCl (10 g/L). The pH was adjusted to 7.0 with NaOH.

Selective medium 1: KNO_3 (1.0 g/L), KH_2PO_4 (0.75 g/L), NaCl (0.75 g/L), $MgSO_4 \cdot 7H_2O$ (0.75 g/L), $FeSO_4 \cdot 7H_2O$ (0.03 g/L), CBT-diol (0.3 g/L), and maltose (2.5 g/L). Maltose is added as an auxiliary carbon source during the initial enrichment stage and promotes the formation of key aroma substances such as solanone.

Solid selective medium: prepared by adding 15 g/L agar powder to the selective medium 1.

1.2 Isolation and purification of strain

Flue-cured tobacco leaf samples (5 g each) from different varieties were cut into fragments and immersed in sterile Erlenmeyer flasks containing 100 mL of sterile water, followed by standing overnight at room temperature. Subsequently, 1 mL of the extract was transferred to conical flasks with 100 mL of LB medium, and enrichment culture was conducted in a constant-temperature shaker at 30 ℃ and 150 r/min for 24 h to obtain enriched strain suspensions. A 1 mL aliquot of the aforementioned strain suspension was inoculated into 100 mL of the selective medium 1. After 4–6 d of expanded culture, metabolites were analyzed by gas chromatography-mass spectrometry (GC-MS) to initially screen for strain communities with potential CBT-diol degradation capacity.

The target strain communities were serially diluted and inoculated onto the surface of the solid selective medium using the spread plate method. The inoculated plates were incubated in a 30 ℃ constant-temperature shaking incubator (THZ-300, Jinan Jinronghui Instrument Technology Co., Ltd., China) for 2–4 d. Single colonies with distinct hydrolysis zones and uniform morphology were preferentially selected for repeated streak purification over multiple generations until axenic monoclonal strains (free of contaminating microorganisms) were obtained.

The purified dominant strains were inoculated into fresh selective medium 1 and cultured for fermentation under the same conditions for 2–4 d. High-efficiency CBT-diol-degrading strains were confirmed by secondary verification via GC-MS. Strain classification was performed based on colonial phenotypic characteristics (e.g., morphology and color). Pure cultures were preserved at −80 ℃, and the dominant strain with the highest abundance was selected for subsequent functional verification experiments.

1.3 Strain identification

1.3.1 Strain morphological characteristics

The strain was streaked on LB agar plates and incubated at 28 ℃ for 48 h, after which its morphological characteristics were observed. The relevant physiological and biochemical indices of the strain were determined with reference to Bergey's Manual of Systematic Bacteriology.

1.3.2 16S rRNA gene amplification, sequencing, and phylogenetic analysis

Using single colonies as templates, we performed PCR amplification of the 16S rRNA gene with universal primers 27F (AGAGTTTGATCCTGGCTCAG) and 1492R (TACGGCTACCTTGTTACGACTT).

The PCR amplification system (total volume: 50 μL) consisted of 25 μL of 2×T3 PCR Mix, 1 μL each of forward and reverse primers (10 μmol/L), and double-distilled water to make up the final volume. The PCR cycling conditions were as follows: initial denaturation at 98 ℃ for 5 min; 35 cycles of denaturation at 98 ℃ for 1.0 min, annealing at 55 ℃ for 1.0 min, and extension at 72 ℃ for 1.5 min; final extension at 72 ℃ for 5.0 min. After verification by electrophoresis, the PCR products were sent to Tsingke Biotechnology

Co., Ltd. China, for sequencing. The obtained gene sequences were submitted to the GenBank database for homology comparison, and a phylogenetic tree was constructed using the neighbor-joining method in MEGA X software[17].

1.4 Analysis of biological characteristics

1.4.1 Determination of optimal temperature, shaking speed, and inoculum size

The strain concentration was standardized to 1.0×10^7 CFU/mL using the turbidimetric method, and the strain suspension was transferred to sterile broth medium at a volume ratio of 1 ∶ 100. Different culture temperatures, shaking speeds, and inoculum sizes were set to investigate their effects on strain growth. Each group was performed with three replicates, and blank medium was used as the control group. A spectrophotometer was employed to measure the optical density of the culture broth at a wavelength of 600 nm (OD_{600}), and growth curves were plotted to determine the optimal growth conditions.

1.4.2 Acid-base tolerance test of strain

Ten test tubes were prepared, each containing 4.9 mL of LB medium. The pH of the medium was adjusted to 5.0, 6.0, 7.0, 8.0, and 9.0, respectively. Then, 100 μL of the strain suspension was added to each tube, followed by thorough mixing. The tubes were incubated at 35 ℃ for 12 h, with three parallel replicates per group and blank medium as the control group. A spectrophotometer was used to measure the OD_{600} of samples. The measured values were recorded, and a pH stability curve was plotted.

1.5 Analysis of degradation characteristics of strain

A single colony of the strain was inoculated into LB medium and cultured under specified conditions (temperature, shaking speed, and pH). The culture was adjusted to the strain suspension with an OD_{600} value of 0.6[18] and then inoculated into the selective medium 1 at a volume fraction of 4%. The CBT-diol degradation efficiency of the fermentation broth was determined at different incubation time points: 8, 16, 24, 32, 40, 48, 56, 64, 72, and 80 h. To ensure the accuracy and reproducibility of the results, three independent parallel experiments were performed. The average values were calculated, and the growth curve of the strain over 80 h was plotted.

1.6 Orthogonal experiment and response surface methodology

In this experiment, through careful planning and organization, a rational experimental design was adopted, and multiple rounds of experiments were conducted strictly to obtain a series of accurate data. Subsequently, a multiple quadratic regression equation was employed to precisely fit the functional relationship between each factor and the response value, ensuring the accuracy and reliability of the analysis results. By conducting an in-depth analysis of the regression equation, the optimal process parameters were effectively explored and determined.

Response surface methodology is a statistical method widely adopted to solve multivariable problems[19]. Its core idea is to accurately approximate the implicit limit state function using polynomial functions through a series of well-designed deterministic experiments.

1.7 Changes in substance content in tobacco leaf concentrate

Thirty milliliters of tobacco leaf concentrate was placed in a 100 mL Erlenmeyer flask, inoculated with 4% (volume fraction) inoculum, and cultured at 30 ℃ with shaking at 150 r/min for 24 h. After incubation, the fermentation broth was transferred to a separatory funnel, and an equal volume of methyl tert-butyl ether/*n*-hexane (a volume ratio of 1 ∶ 1) mixed solvent was added for liquid-liquid extraction. This extraction process was repeated three times, and the obtained organic phases were combined. An appropriate amount of anhydrous sodium sulfate was added to the combined organic phase for overnight dehydration. Subsequently, the solvent was removed by rotary evaporation. α-Ionone was added as an internal standard to the resulting residue, which was then filtered through a 0.45 μm organic phase filter membrane. GC-MS was used to analyze and compare the changes in the composition and content of flavor substances in the samples before and after fermentation.

1.8 GC-MS

GC-MS was conducted by an Agilent 6890a/5975c GC-MS system (Agilent Technologies, USA).

The gas chromatography (GC) conditions were as follows. The chromatographic column was a DB-5MS capillary column (30 m × 0.25 mm × 0.25 μm). Carrier gas was helium (purity ≥ 99.999%). Flow rate was 2 mL/min in constant flow mode. The injection port was maintained at 50 ℃ for 0.1 min, then the temperature was raised to 250 ℃ at a rate of 500 ℃/min and held for 5 min, followed by heating up to 350 ℃ at a rate of 500 ℃/min and maintained for 20 min. The temperature program was set as follows. The temperature was first kept at 40 ℃ for 3 min, heated to 100 ℃ at a rate of 10 ℃/min, then increased to 250 ℃ at 3 ℃/min and held for 1 min, and finally raised to 300 ℃ at a rate of 20 ℃/min and maintained for 20 min.

The mass spectrometry (MS) conditions were as follows. Interface temperature was 230 ℃. Electron energy was 70 eV. EI source temperature was 230 ℃. Quadrupole temperature was 150 ℃. Mass scanning range was 33–500 atomic mass units.

1.9 Calculation of degradation efficiency

The degradation efficiency of CBT-diol was calculated according to the following formula:

$$\eta = \frac{C_0 - C_t}{C_0} \times 100\%,$$

where η is the degradation efficiency of CBT-diol; C_0 is

the initial concentration ($t=0$); C_t is the concentration at time t.

2 Results and Discussion

2.1 Results of strain isolation and purification

One CBT-diol-degrading strain was isolated from tobacco leaves and designated as Z1-1. This strain was inoculated into the selective medium 1 for selective cultivation. As shown in Fig. 1, the strain formed yellow, convex colonies with a moist and smooth surface on LB agar plates. Gram staining results (Fig. 2) indicated that the strain was Gram-negative.

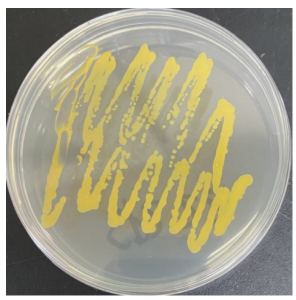


Fig. 1 Colony morphology

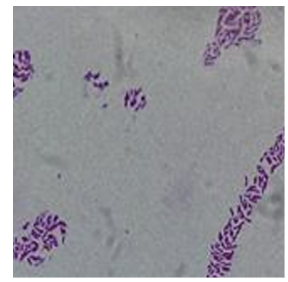


Fig. 2 Gram staining

2.2 16S rRNA gene sequencing and phylogenetic analysis of the strain

Based on 16S rRNA gene sequencing and phylogenetic analysis, strain Z1-1 shared a sequence homology of over 99% with members of the genus *Novosphingobium* retrieved from the GenBank database. Phylogenetic tree results (Fig. 3) showed that the strain clustered with members of the genus *Novosphingobium* into a stable evolutionary clade, supporting its classification within this genus. In particular, the evolutionary branch formed by strain Z1-1 and *Novosphingobium lubricantis* has received strong statistical support, with a bootstrap value reaching 99%. This provides strong evidence for its classification within the genus.

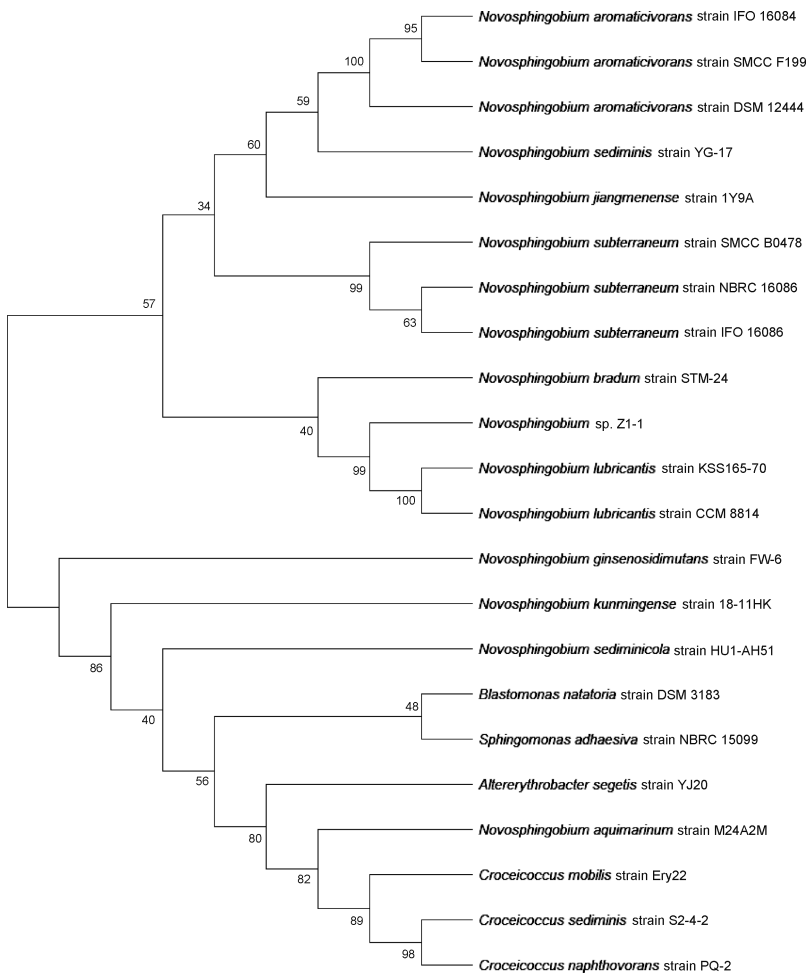


Fig. 3 Phylogenetic tree

Bacteria of the genus *Novosphingobium* are widely distributed in natural environments and exhibit the ability to degrade various organic pollutants, such as polycyclic aromatic hydrocarbons (PAHs) and pesticides. Despite the high conservation of their 16S rRNA sequences, bacteria in this genus display significant diversity in metabolic functions, which may be associated with their adaptive evolution in different ecological niches.

Combining the results of morphological observations and phylogenetic analysis, strain Z1-1 was tentatively identified as *Novosphingobium* sp. This taxonomic identification not only provides a taxonomic basis for its CBT-diol degradation capacity but also suggests that the strain may possess other metabolic potentials related to environmental adaptability.

2.3 Analysis of biological characteristics

2.3.1 Effects of temperature and shaking speed on strain growth

As shown in Fig. 4(a), the biomass of the strain showed an upward trend under all three temperature conditions, with relatively similar growth patterns. Among them, the 35 ℃ treatment group exhibited the fastest biomass accumulation rate, and the final biomass was significantly higher than that under other temperature conditions. This indicates that 35 ℃ is most conducive to the function of the strain's enzyme system and can be regarded as its optimal growth temperature. Temperature influences strain growth mainly by regulating enzyme activity, cell membrane fluidity, and nutrient absorption efficiency. Low temperatures slow down metabolic rates, while high temperatures may cause denaturation and inactivation of enzyme proteins. The temperature range of 30–35 ℃ is close to the natural environmental temperature on plant surfaces, suggesting that strain Z1-1 has good physiological adaptability to its original habitat.

As indicated in Fig. 4(b), the trends of the strain's growth kinetic curves were basically consistent under different shaking speed conditions. The biomass reached the highest at 150 r/min, demonstrating that this shaking speed is the optimal culture condition. Shaking speed affects strain growth primarily by altering dissolved oxygen (DO) levels and the uniformity of medium mixing. Excessively low shaking speeds lead to insufficient DO supply and uneven distribution of nutrients, while excessively high shaking speeds may cause mechanical damage to strain cells due to fluid shear stress. Since Z1-1 is an aerobic bacterium, both its aerobic respiration and CBT-diol degradation processes rely on an adequate oxygen supply. The shaking speed of 150 r/min provides the optimal gas-liquid mass transfer conditions for the strain.

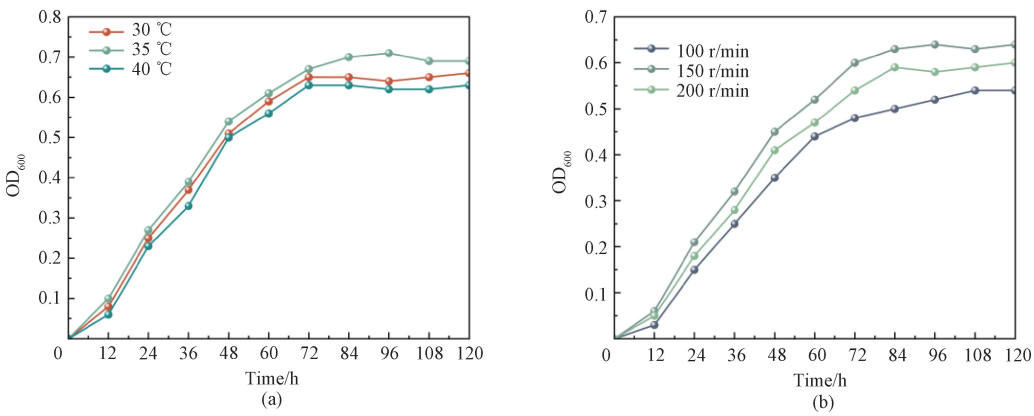


Fig. 4 Effects of temperature and shaking speed on strain biomass: (a) growth curves of the strain at different temperatures; (b) growth curves of the strain at different shaking speeds

2.3.2 Effects of inoculum size on strain growth

As shown in Fig. 5, the growth curves of the strain exhibited essentially consistent trends under different inoculum sizes. Among all treatments, the 4% (volume fraction) inoculum size yielded the highest final biomass, indicating that this condition is the optimal inoculum size for strain Z1-1. The final biomass values of the 3% and 5% (volume fraction) inoculum groups were each relatively similar but still lower than that of the 4% (volume fraction) group.

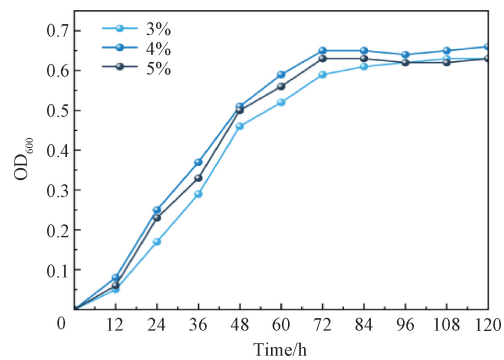


Fig. 5 Effects of initial inoculum size on strain biomass

An appropriate inoculum size facilitates the establishment of a sufficient initial strain density, promoting quorum sensing and synergistic metabolic behaviors. An excessively low inoculum size delays the process of microbial community establishment, while an excessively high inoculum size may lead to intensified nutrient competition and accumulation of metabolic by-products, thereby inhibiting strain growth. These results provide key parameters for optimizing large-scale fermentation processes and contribute to the achievement of efficient biotransformation.

2.3.3 Effects of pH on strain growth

As shown in Fig. 6, the growth performance of strain Z1-1 varied significantly under different initial pH conditions. In the acidic environment of pH 5.0, strain growth was significantly inhibited, with extremely limited biomass accumulation. Under the alkaline condition of pH 9.0, the strain growth was moderately improved but still failed to reach the optimal state. The optimal growth pH range was determined to be 7.0–8.0, where the neutral environment facilitated the highest biomass accumulation, indicating that the strain's enzyme system exhibits maximum activity within this pH range. pH primarily regulates metabolic activity by influencing enzyme proteins; extreme pH conditions may disrupt cell membrane integrity and interfere with transmembrane substance transport processes. The pH of tobacco leaf surfaces is typically near neutral, and the adaptability of strain Z1-1 to neutral pH further reflects the high matching degree between its physiological characteristics and the original ecological environment.

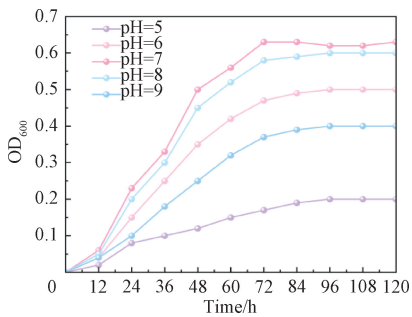


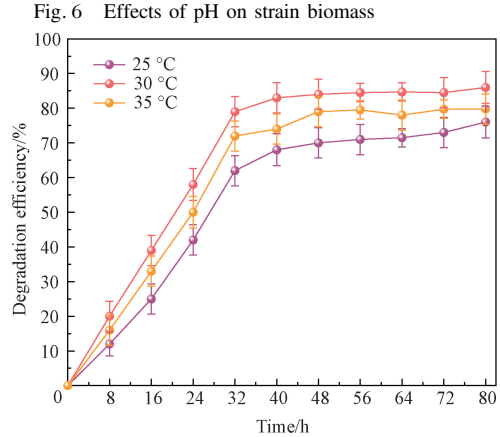
Fig. 6 Effects of pH on strain biomass

2.4 Degradation characteristics of strain

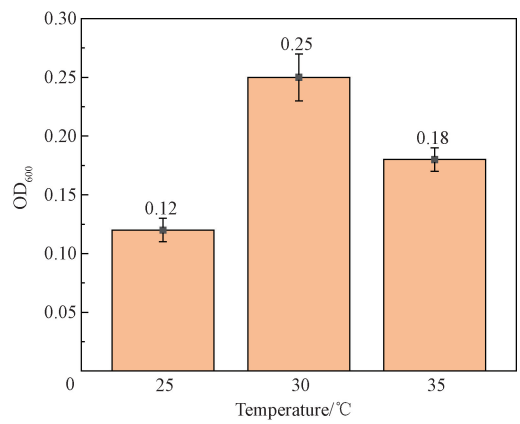
2.4.1 Effects of temperature on degradation efficiency

As illustrated in Fig. 7, temperature exerted a significant influence on both the CBT-degrading capacity and growth of strain Z1-1. Figure 7(a) shows that at 30 ℃, the CBT degradation efficiency was the fastest, with the degradation efficiency exceeding 80% after approximately 40 h of cultivation, which indicated the onset of the stationary phase. This time point was thus selected as it accurately captures the transition to the plateau phase in the degradation kinetics, representing the period of maximum degradation activity before stabilization. In contrast, both the degradation efficiency and final degradation efficiency were significantly lower at 25 ℃ and 35 ℃, indicating that the degradation process is a typical growth-associated metabolism. Temperature not only directly affects the structure and catalytic activity of degrading enzymes but also regulates cell membrane fluidity, thereby influencing the transmembrane transport efficiency of hydrophobic substrates such as CBT-diol. Excessively low temperatures reduce reaction rates, while excessively high temperatures may cause denaturation and inactivation of enzyme proteins.

Figure 7(b) further demonstrates that after 80 h of cultivation, the final biomass of the 30 ℃ treatment group reached its peak, whereas the biomass values at 25 ℃ and 35 ℃ were each only approximately half of this peak value. This finding further confirms the close correlation between strain growth and degradation efficiency. Thus, temperature regulates the CBT-diol degradation process through a dual mechanism: on the one hand, it directly modulates the activity of key enzymes; on the other hand, it indirectly determines the overall degradation capacity of the system by influencing the strain growth status. A temperature of 30 ℃ was identified as optimal for strain Z1-1, under which its enzymatic system function, membrane structural integrity, and cellular metabolic activity all reached their best states.



(a)



(b)

Fig. 7 Effects of temperature on CBT-diol degradation efficiency and strain biomass: (a) CBT-diol degradation efficiency; (b) strain biomass after 80 h of cultivation

We speculate that the key enzyme system responsible for initiating the degradation of CBT-diol may exhibit higher catalytic efficiency or conformational stability at 30 ℃ than that at 35 ℃. At 35 ℃, although the bacteria grow rapidly, some of the energy may be used to cope with thermal stress, resulting in relatively insufficient resources for synthesizing the degradation enzymes. However, at 30 ℃, the metabolism is more stable, and the energy can be more specifically allocated to the CBT-diol degradation pathway. A temperature of 30 ℃ appears to be optimal for hydrophobic CBT-diol molecules to traverse the cell membrane, thereby ensuring efficient substrate uptake.

2.4.2 Effects of shaking speed on degradation efficiency

As illustrated in Fig. 8, shaking speed exerted a significant influence on both the CBT-diol degradation efficiency and growth of strain Z1-1. Figure 8(a) shows that at 150 r/min, the CBT-diol degradation efficiency was the fastest, and the final degradation efficiency also reached the highest level. When the shaking speed decreased to 100 r/min, both the degradation efficiency and the final degradation efficiency decreased significantly. In contrast, the degradation efficiency was the lowest at 0 r/min and 200 r/min, indicating a non-linear regulatory effect of shaking speed on the degradation process. The lowest degradation efficiency was recorded under static culture conditions (a shaking speed of 0 r/min), which was deliberately introduced to simulate an oxygen-deficient environment. This result confirms that severe limitation of oxygen supply will greatly hinder the degradation process.

Figure 8(b) demonstrates that the final strain biomass was relatively high at 150 r/min and 200 r/min, decreased at 100 r/min, and was limited at 0 r/min. This indicates that moderate DO levels and mixing conditions are critical for the normal growth of the strain. Shaking speed regulates the degradation process primarily by influencing oxygen transfer efficiency, the uniformity of medium mixing, and the contact frequency between CBT and strain cells. Excessively low shaking speeds lead to insufficient DO supply and mass transfer limitations, thereby affecting aerobic metabolism and substrate availability. Conversely, excessively high shaking speeds may cause mechanical damage to strain cells due to fluid shear stress.

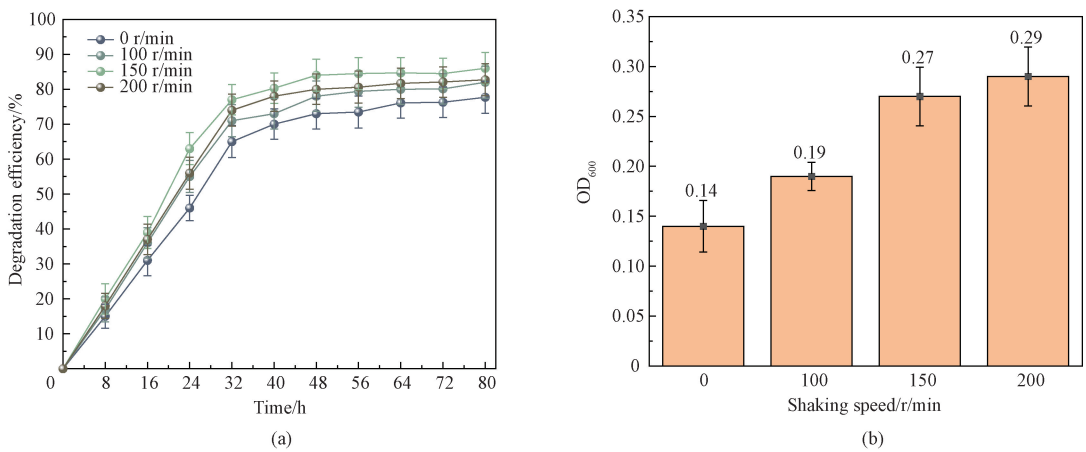


Fig. 8 Effects of shaking speed on CBT-diol degradation efficiency and strain biomass: (a) degradation efficiency; (b) strain biomass after 80 h of cultivation

Collective results indicate that 150 r/min is the optimal shaking speed for both CBT-diol degradation and growth of strain Z1-1. Under static conditions, growth is severely inhibited. This shaking speed not only provides an adequate oxygen supply but also achieves favorable mixing effects and low shear stress, thereby promoting strain growth while ensuring efficient CBT-diol degradation.

2.4.3 Effects of pH on degradation efficiency

As illustrated in Fig. 9, the initial pH exerted a significant influence on both the CBT-diol degradation efficiency and the growth of strain Z1-1. As shown in Fig. 9(a), at pH 7.0, the kinetic curve of CBT-diol degradation exhibited the steepest slope, corresponding to the fastest degradation efficiency and the highest final degradation efficiency. When the pH was higher than 7.0 or lower than 6.0, both the degradation efficiency and rate gradually decreased. Under acidic (pH 5.0) conditions, the degradation process was significantly inhibited. Figure 9(b) further demonstrates that the strain biomass reached its peak within a pH range of 7.0–8.0, while growth was inhibited to varying degrees at pH 5.0, 6.0, and 9.0. This indicates that both strain growth and degradation capacity are dependent on an optimal pH environment.

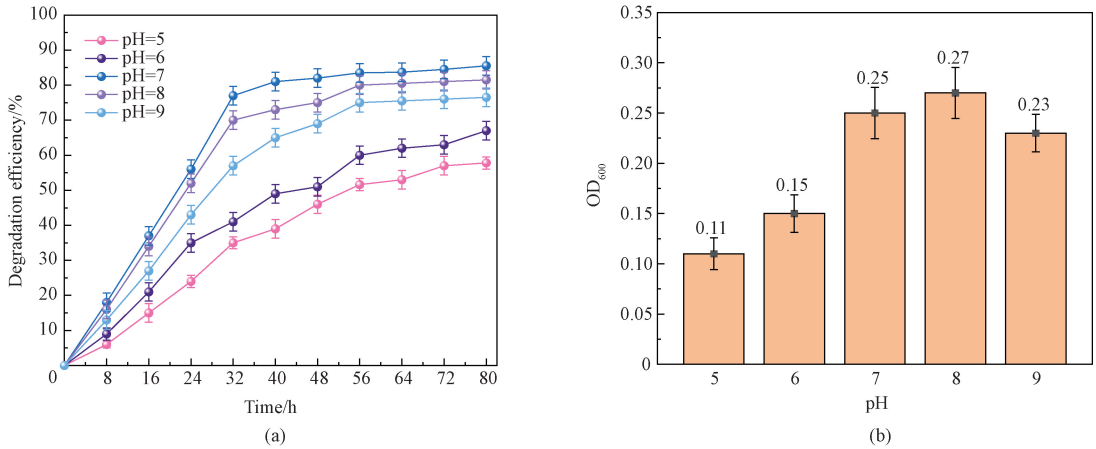


Fig. 9 Effects of pH on CBT degradation efficiency and strain biomass: (a) CBT-diol degradation efficiency; (b) strain biomass after 80 h of cultivation

The optimal pH for the CBT-diol degrading enzyme system of strain Z1-1 is likely around neutrality, where enzymatic catalytic activity is maximized. A suitable pH environment helps maintain the integrity of cell membrane structure and function, ensuring the stability of transmembrane proton gradients and the normal operation of energy metabolism[20]. Extreme pH conditions may not only cause inactivation of key metabolic enzymes and disrupt central metabolic pathways but also alter the solubility of nutrients, thereby reducing their bioavailability. The aforementioned results indicate that pH synergistically regulates the degradation performance and growth behavior of strain Z1-1 through multiple mechanisms.

2.5 Results of orthogonal experiment and response surface methodology

2.5.1 Orthogonal experiment analysis

Based on the results of the three single-factor experiments (temperature, shaking speed, and pH), the level range of each factor in the uniform experiment was further clarified. Taking the CBT-diol degradation efficiency as the response value, an orthogonal experiment was conducted, and the experimental design and results are shown in Table 1.

Table 2 shows the results of analysis of variance (ANOVA). As shown in Table 2, the quadratic regression model was highly significant ($F = 93.59$, $p < 0.0001$). pH (Factor C) was the most influential factor, with both linear and quadratic terms being extremely significant ($p < 0.0001$). Temperature (Factor A) and shaking speed (Factor B) both showed significant nonlinear effects ($p = 0.0002$ and $p = 0.0018$ for their quadratic terms, respectively), while their linear effects were not significant. No significant interactions were observed between any pair of factors. The non-significant lack of fit ($p = 0.0749$) and small pure error (4.48) indicated that the model fitted the experimental data well and could be used for prediction.

Table 1 Experimental design and results

Serial number	Temperature/℃ (Factor A)	Shaking speed/(r/min) (Factor B)	pH (Factor C)	CBT-diol degradation efficiency /%
1	30	150	7.0	83.9
2	25	100	7.0	73.7
3	35	150	5.0	47.2
4	30	150	7.0	86.2
5	25	200	7.0	73.1
6	35	100	7.0	73.2
7	30	200	5.0	54.3
8	30	100	5.0	49.3
9	30	150	7.0	85.3
10	30	100	9.0	74.8
11	30	150	7.0	86.1
12	30	150	7.0	84.2
13	30	200	9.0	73.8
14	35	200	7.0	78.5
15	25	150	9.0	72.3
16	25	150	5.0	52.9
17	35	150	9.0	71.3

Table 2 ANOVA results

Source	Sum of squares	Degree of freedom	Mean square	F	p
Model	2602.735	9	289.19	93.59	< 0.000 1
A	0.405	1	0.405	0.130 9	0.728 2
B	9.46	1	9.46	3.06	0.1238
C	979.03	1	979.03	316.48	< 0.000 1
AB	8.7	1	8.7	2.81	0.137 4
AC	5.52	1	5.52	1.79	0.223 3
BC	9	1	9	2.91	0.1318
A^2	168.18	1	168.18	54.37	0.000 2
B^2	74.1	1	74.1	23.95	0.001 8
C^2	1348.34	1	1 348.34	436.52	< 0.000 1
Residual	21.63	7	3.09		
Lack of fit	17.16	3	5.72	5.09	0.074 9
Pure error	4.48	4	1.12		

2.5.2 Response surface plot analysis

Figure 10 illustrates the effects of pH (Factor C, 5–9) and shaking speed (Factor B, 100–200 r/min) on CBT-diol degradation efficiency while the temperature is kept constant (at 30 ℃). From the surface morphology, the degradation efficiency reaches a peak around pH 7 and gradually decreases toward both sides. Particularly, the degradation efficiency drops significantly to below 50% at pH 5, which is consistent with the ANOVA result that both the linear and quadratic terms of pH are highly significant ($p < 0.000\,1$).

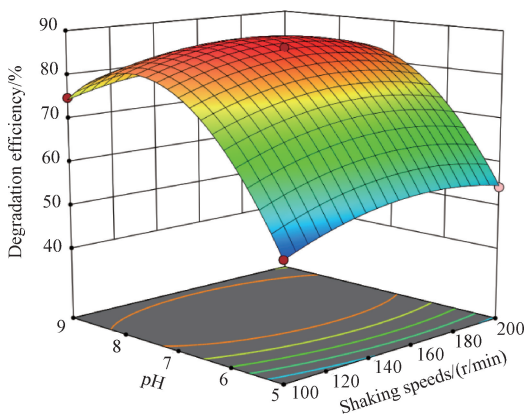


Fig. 10 Response surface plot of the effects of pH and shaking speed on CBT-diol degradation efficiency

The change in shaking speed has a relatively weak impact on the degradation efficiency, but the surface plot shows a slightly higher degradation efficiency around 150 r/min, which aligns with the significant quadratic term of shaking speed in the ANOVA. The overall surface is convex, indicating a slight synergistic effect between pH and shaking speed. However, the interaction term (BC) is not significant in the ANOVA ($p = 0.131\,8$), so this effect may mainly stem from their respective main effects and nonlinear components. The optimal region appears around pH 7 and 150 r/min, which is consistent with the central point conditions of the experiment.

Figure 11 shows the effects of pH (Factor C, 5–9) and temperature (Factor A, 25 – 35 ℃) on CBT degradation efficiency while shaking speed is kept constant (likely at 150 r/min). The response surface exhibits a distinct peak at approximately 85% – 86% around pH 7 and 30 ℃. As pH deviates from neutrality or temperature departs from 30 ℃, the degradation efficiency decreases.

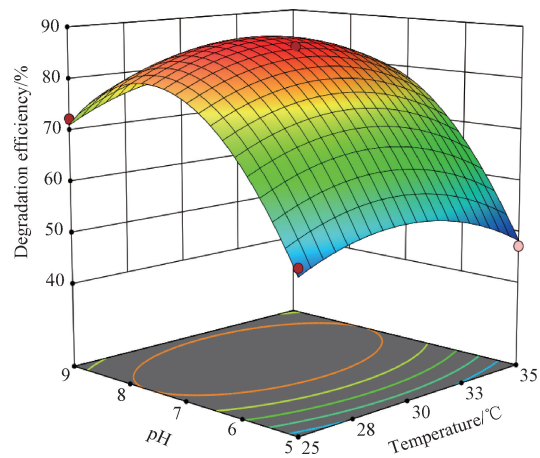


Fig. 11 Response surface plot of the effects of pH and temperature on CBT-diol degradation efficiency

The impact of pH is particularly prominent: the degradation efficiency drops to below 75% at pH 5 or 9, revalidating pH as the most critical factor. The effect of temperature presents a nonlinear characteristic: within 25 –35 ℃, the degradation efficiency first increases and then decreases. This is consistent with the ANOVA results, where the quadratic term of temperature is highly significant, but the linear term is not.

The surface morphology is smooth without obvious distortion, indicating a weak interaction between pH and

temperature, which aligns with the statistical results. Figure 11 emphasizes that maintaining pH 7 and 30 ℃ is crucial for maximizing CBT-diol degradation efficiency in process optimization.

Figure 12 depicts the effects of shaking speed (Factor B, 100–200 r/min) and temperature (Factor A, 25–35 ℃) on CBT-diol degradation efficiency while pH is kept constant. The response surface presents a relatively flat hilly shape, with a peak appearing around 150 r/min and 30 ℃, where the degradation efficiency reaches approximately 85%–86%.

As the shaking speed or temperature deviates from the central point, the degradation efficiency gradually decreases, but with a small variation range. For example, the degradation efficiency drops to 70%–80% at 100 or 200 r/min, and a similar trend is observed at 25 ℃ or 35 ℃. This reflects the nonlinear effects of shaking speed and temperature, while their linear effects are weak.

The contour lines of the surface are roughly symmetric, indicating no strong interaction between shaking speed and temperature, which is consistent with the statistical results. Figure 12 suggests that under the optimal pH condition, minor changes in shaking speed and temperature have limited impacts on the degradation efficiency. However, to achieve the highest efficiency, it is still recommended to control them near the central point.

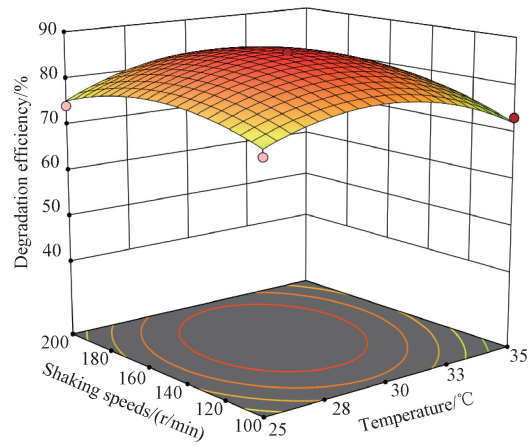


Fig. 12 Response surface plot of the effects of temperature and shaking speed on CBT degradation efficiency

2.6 Changes in aroma compounds in tobacco leaf concentrate

Aroma compounds in tobacco leaf concentrates were analyzed using GC-MS before and after microbial fermentation. As shown in Table 3, strain Z1-1 significantly increased the contents of multiple key aroma-active compounds. Specifically, the relative contents of solanone, 9-hydroxy-4, 7-megastigmat-rienone (9-OH-MGT), 4-hydroxy-β-damascone (4-OH-β-Dam), and phytol increased to 7.22, 3.65, 1.79, and 3.80 times their original levels. These results demonstrate the strain's excellent aroma-producing potential.

Table 3 Changes in aroma compound contents in tobacco leaf concentrate before and after fermentation

Serial number	Retention time/min	Compound	Relative content/%	
			Before fermentation	After fermentation
1	19.1	Solanone	1.012	7.303
2	28.7	9-OH-MGT	2.919	10.662
3	31.5	4-OH-β-Dam	2.014	3.597
4	43.8	Phytol	5.124	19.458

Based on the marked increase in key aroma compounds such as solanone, the study postulated that strain Z1-1 potentially converted CBT-diol into these aroma-active molecules via specific enzymatic reactions. The proposed biochemical pathway involved initial selective hydroxylation or peroxidation of the CBT-diol skeleton, likely catalyzed by cytochrome P450 monooxygenases or dioxygenases. Subsequently, unstable intermediates underwent oxidative cleavage of C—C bonds, potentially mediated by lyase-like enzymes, followed by further modifications catalyzed by dehydrogenases to yield low-molecular-weight terpenoid aroma compounds, including solanone. This proposed transformation mechanism aligned with previously reported microbial ring-opening degradation pathways for terpenoids[21].

3 Conclusions

A bacterial strain designated Z1-1, capable of utilizing CBT-diol as its primary carbon source and degrading it efficiently, was successfully isolated from flue-cured tobacco leaves. Morphological observation, physiological and biochemical characteristics, and 16S rRNA gene sequence analysis led to the preliminary identification of the strain as *Novosphingobium* sp.

Systematic optimization of culture conditions established the optimal growth and degradation parameters for strain Z1-1 as a temperature of 30 ℃, a shaking speed of 150 r/min, an inoculum size of 4%, and an initial pH of 7.0[22]. Under these optimized conditions, a high

CBT-diol degradation efficiency of 83.47% was achieved within 36 h of cultivation. Furthermore, the specific addition of maltose to the medium directionally promoted the synthesis of the key aroma compound solanone, indicating the regulatable nature of the strain's metabolic pathways.

Application trials in tobacco leaf concentrate demonstrated that inoculation with strain Z1-1 significantly enhanced the relative contents of multiple key neutral aroma compounds. Specifically, the relative contents of solanone, 9-OH-MGT, 4-OH-β-Dam, and phytol increased to 7.22, 3.65, 1.79, and 3.80 times their original levels, respectively. These results confirm the clear potential of this strain for application in microbial technology aimed at supplementing the aroma profile and improving the aroma quality of tobacco products.

In summary, *Novosphingobium* sp. Z1-1 not only provides an excellent model organism for elucidating the microbial degradation mechanism of cembranoid compounds but also exhibits significant biocatalytic potential due to its efficient degradation and targeted aroma-enhancing properties. The application of this strain offers a novel technical strategy for the safe and efficient improvement of the intrinsic quality of tobacco and other tobacco products, demonstrating broad prospects for industrial application. Future research should focus on the isolation, purification, and catalytic mechanism analysis of its key degrading enzymes, as well as the optimization and scale-up of large-scale fermentation processes.

References

[1] Xu K, Du X Y, Ren X, et al. Structural modifications and biological activities of natural α- and β-cembrenediol: a comprehensive review [J]. *Pharmaceuticals*, 2022, 15(5): 601.

[2] Yan B W, Jia H J, Wei J H, et al. Extraction, purification and anti-TMV effects of α (β)-2, 7, 11-cembratriene-4, 6-diol from tobacco leaves [J]. *Industrial Crops and Products*, 2021, 174: 114197.

[3] Sui J K, Wang C K, Liu X F, et al. Formation of α- and β-cembratriene-4, 6-diols in tobacco (*Nicotiana tabacum* L.) is regulated by jasmonate-signaling components via manipulating multiple cembranoid synthetic genes [J]. *Molecules*, 2018, 23(10): 2511.

[4] Ferchmin P A, Andino M, Reyes Salaman R, et al. 4*R*-cembranoid protects against diisopropylfluorophosphate-mediated neurodegeneration [J]. *NeuroToxicology*, 2014, 44: 80-90.

[5] Hu J, Ferchmin P A, Hemmerle A M, et al. 4*R*-cembranoid improves outcomes after 6-hydroxydopamine challenge in both in vitro and in vivo models of Parkinson's disease [J]. *Frontiers in Neuroscience*, 2017, 11: 272.

[6] Martins A H, Hu J, Xu Z, et al. Neuroprotective activity of (1*S*, 2*E*, 4*R*, 6*R*, -7*E*, 11*E*)-2, 7, 11-cembratriene-4, 6-diol (4*R*) in vitro and in vivo in rodent models of brain ischemia [J]. *Neuroscience*, 2015, 291: 250-259.

[7] Sabeva N, Pagán O R, Ferrer-Acosta Y, et al. In vivo evaluation of the acute systemic toxicity of (1*S*, 2*E*, 4*R*, 6*R*, 7*E*, 11*E*)-cembratriene-4, 6-diol (4*R*) in sprague dawley rats [J]. *Nutraceuticals*, 2022, 2(2): 60-70.

[8] Sabeva N, Castro W, Acosta Y F, et al. Determining the safety of the tobacco cembranoid (1*S*, 2*E*, 4*R*, 6*R*, 7*E*, 11*E*)-cembratriene-4, 6-diol (4*R*): a translational study in nonhuman primates [J]. *Toxicology and Applied Pharmacology*, 2024, 482: 116772.

[9] Ebrahim H Y, Mohyeldin M M, Hailat M M, et al. (1*S*, 2*E*, 4*S*, 7*E*, 11*E*)-2, 7, 11-cembratriene-4, 6-diol semisynthetic analogs as novel c-Met inhibitors for the control of c-Met-dependent breast malignancies [J]. *Bioorganic & Medicinal Chemistry*, 2016, 24(22): 5748-5761.

[10] Bai B, Wang L, Xu G G, et al. Synthesis and antitumor activities of α-2,7,1-cembratriene-4.6-diol derivatives[J]. *Chemical Journal of Chinese Universities*, 2020, 41(3): 481-489. (in Chinese)

[11] Jia C X, He F, Ma Y P, et al. Research advance in cembranoid compounds[J]. *Journal of Light Industry*, 2016, 31(1): 46-54. (in Chinese)

[12] Kang H L, Liu X R, Zhao S S, et al. Study on degradation of Chifeng lignite of Inner Mongolia by four kinds of bacteria[J]. *Coal Technology*, 2019, 38(10): 130-133. (in Chinese)

[13] Zhang Y L, Gao C H, Jin D S, et al. Analysis of decomposing performance of *Sphingomonas* in promoting straw decomposition in reclaimed soil of mining area [J]. *Journal of Shanxi Agricultural Sciences*, 2022, 50(1): 67-77. (in Chinese)

[14] Zhang X M, Li B, Yan H Y, et al. Effects of nitrogen sources addition on bacterial communities and their degradation of petroleum hydrocarbons in oil-based drilling cuttings[J]. *Chinese Journal of Environmental Engineering*, 2024, 18(6): 1624-1637. (in Chinese)

[15] Yan N, Du Y M, Liu X M, et al. A review on bioactivities of tobacco cembranoid diterpenes [J]. *Biomolecules*, 2019, 9(1): 30.

[16] Huang S, Huo M J, Qian Y M, et al. Screening and identification of a cembratriene-4, 6-diol degradating strain and its application in reconstituted tobacco [J]. *Journal of Henan Agricultural Sciences*, 2018, 47(10): 137-142, 148. (in Chinese)

[17] Kumar S, Stecher G, Li M, et al. MEGA X: molecular evolutionary genetics analysis across computing platforms [J]. *Molecular Biology and Evolution*, 2018, 35(6): 1547-1549.
[18] Yuan X Y, Zhang X Y, Chen X P, et al. Synergistic degradation of crude oil by indigenous strain consortium and exogenous fungus *Scedosporium boydii* [J]. *Bioresource Technology*, 2018, 264: 190-197.
[19] Zhao J Y, Lyu L Y, Han X Y, et al. Screening and taxonomic characterization of the efficient flocculating bacterium EbZL-1 and its application in microalgae harvesting[J]. *Journal of Donghua University* (*English Edition*), 2024,41(1): 46-56.
[20] Olaniran A O, Babalola G O, Okoh A I. Aerobic dehalogenation potentials of four strain species isolated from soil and sewage sludge [J]. *Chemosphere*, 2001, 45(1): 45-50.
[21] Bicas J L, Dionísio A P, Pastore G M. Bio-oxidation of terpenes: an approach for the flavor industry [J]. *Chemical Reviews*, 2009, 109(9): 4518-4531.
[22] An T C, Zu L, Li G Y, et al. One-step process for debromination and aerobic mineralization of tetrabromobisphenol-A by a novel *Ochrobactrum* sp. T isolated from an e-waste recycling site [J]. *Bioresource Technology*, 2011, 102(19): 9148-9154.

降解西柏三烯二醇产香的新鞘氨醇杆菌菌株：分离、鉴定及生物学特性

邵 霞[1]，王嘉乐[2]，吴 达[2]，张 哲[1]，孙 悦[1]，邢佳怡[1]，沙云菲[2*]

1. 上海应用技术大学，上海 201418
2. 上海烟草集团有限责任公司，卷烟烟气重点实验室，上海 200082

摘　要：为获得能够高效降解西柏三烯-4,6-二醇（cembratriene-4,6-diol，CBT-diol）从而提升烟草香气品质的细菌菌株，以 CBT-diol 为唯一碳源，从烟叶中分离筛选出一株目标菌株，命名为 Z1-1。根据形态学特征、生理生化特性及 16S rRNA 基因序列分析，该菌株为新鞘氨醇杆菌属（*Novosphingobium* sp.）。通过单因素试验和响应面法优化其降解条件，确定最佳降解条件：温度 30 ℃、摇床转速 150 r/min、接种量 4%、pH 7.0。在此优化条件下，36 h 内 CBT-diol 的降解率达 83.47%。将该菌株应用于烟草浓缩液中，显著提升了多种关键香气成分的相对含量：茄酮、9-羟基-4,7-巨豆三烯酮、4-羟基-β-大马酮和植醇的相对含量分别为原含量的 7.22 倍、3.65 倍、1.79 倍和 3.80 倍。这些结果表明，新鞘氨醇杆菌 Z1-1 是一株高效的 CBT-diol 降解产香菌。

关键词：西柏三烯二醇；新鞘氨醇杆菌属；系统发育分析；分离鉴定；降解